THE JOURNAL OF BIOLOGICAL CHEMISTRY
Vol. 280, No. 32, Issue of August 12, pp. 29080–29087, 2005

Printed in U.S.A.

Human Serum IgM Glycosylation

IDENTIFICATION OF GLYCOFORMS THAT CAN BIND TO MANNAN-BINDING LECTIN*

Received for publication, April 26, 2005, and in revised form, May 31, 2005
Published, JBC Papers in Press, June 14, 2005, DOI 10.1074/jbc.M504528200

James N. Arnold‡, Mark R. Wormald§, David M. Suter§, Catherine M. Radcliffe§, David J. Harvey§, Raymond A. Dwek§, Pauline M. Rudd§, and Robert B. Sim‡¶

From the ‡Medical Research Council Immunochemistry Unit and the §Oxford Glycobiology Institute, Department of Biochemistry, University of Oxford, South Parks Road, Oxford OX1 3QU, United Kingdom

The glycoprotein IgM is the major antibody produced in the primary immune response to antigens, circulating in the serum both as a pentamer and a hexamer. Pentameric IgM has a single J chain, which is absent in the hexamer. The μ (heavy) chain of IgM has five *N*-linked glycosylation sites. Asn-171, Asn-332, and Asn-395 are occupied by complex glycans, whereas Asn-402 and Asn-563 are occupied by oligomannose glycans. The glycosylation of human polyclonal IgM from serum has been analyzed. IgM was found to contain 23.4% oligomannose glycans $GlcNAc_2Man_{5–9}$, consistent with 100% occupancy of Asn-402 and 17% occupancy of the variably occupied site at Asn-563. Mannan-binding lectin (MBL) is a member of the collectin family of proteins, which bind to oligomannose and GlcNAc-terminating structures. A commercial affinity chromatography resin containing immobilized MBL has been reported to be useful for partial purification of mouse and also human IgM. Human IgM glycoforms that bind to immobilized MBL were isolated; these accounted for only 20% of total serum IgM. Compared with total serum IgM, the MBL-binding glycoforms contained 97% more GlcNAc-terminating structures and 8% more oligomannose structures. A glycosylated model of pentameric IgM was constructed, and from this model, it became evident that IgM has two distinct faces, only one of which can bind to antigen, as the J chain projects from the non-antigen-binding face. Antigen-bound IgM does not bind to MBL, as the target glycans appear to become inaccessible once IgM has bound antigen. Antigen-bound IgM pentamers therefore do not activate complement via the lectin pathway, but MBL might have a role in the clearance of aggregated IgM.

The glycoprotein IgM is the major antibody produced in the primary immune response to foreign antigens. It exists both as part of the B cell antigen receptor on the surface of B cells and as a secreted glycoprotein. Human secreted IgM is a multimeric molecule consisting of five (pentameric) (Fig. 1) or six (hexameric) 190-kDa subunits, each of which consists of two heavy (μ) and two light chains. Pentameric IgM has also a single 20-kDa J chain, which is absent in hexameric IgM (1). The μ (heavy) chains consist of five Ig domains termed Vμ, Cμ1, Cμ2, Cμ3, and Cμ4. Interchain disulfide bridges occur in the Cμ2, Cμ3, and Cμ4/tail domains at Cys-337, Cys-414, and Cys-575, respectively. Light chains are attached to Cys-136 in the Cμ1 domain. The polymerization of IgM requires Cys-575 (2), located on the 18-residue tail piece, at the C terminus of each Cμ4 domain. In contrast to the Ig domains, the tail piece has no defined secondary or tertiary structure (3), but is required for the polymerization of monomeric IgM (4). The J chain is attached via Cys-14 and Cys-68 to the penultimate amino acid of two μ chains in pentameric IgM (Cys-575) (5–7). In the absence of a J chain during polymerization, cells secrete solely hexameric IgM (8). The J chain also binds to the poly-Ig receptor, which mediates epithelial transcytosis (9).

Human secreted IgM has five *N*-linked glycosylation sites on each μ chain, located at Asn-171, Asn-332, Asn-395, Asn-402, and Asn-563. The J chain contains a single *N*-linked glycosylation site at Asn-48. The light chains (κ or λ) contain no conserved *N*-linked glycosylation sites. Glycosylation is vital to IgM secretion and B cell surface presentation (10). Oligomannose structures have been shown to occupy two *N*-linked sites on IgM at Asn-402 and Asn-563 (11, 12). These oligosaccharides may present a target for serum mannan-binding lectin (MBL).[1]

MBL, also known as mannan/mannose-binding protein, is a member of the collectin family of proteins (13). MBL is synthesized in the liver and secreted into the bloodstream. It binds calcium-dependently to sugars that have hydroxyl groups on C-3 and C-4 orientated in the equatorial plane of the pyranose ring (14). This gives MBL affinity for mannose, fucose, and GlcNAc (15) present on the surfaces of microorganisms, including bacteria, viruses, and fungi (16), but not generally for human glycoprotein glycans, the structures of which usually terminate in galactose or sialic acid. It binds to sugar residues via the carbohydrate recognition domain (lectin) heads. The affinity of a single carbohydrate recognition domain for carbohydrate is very weak (10^{-3} M) (17), but multiple carbohydrate recognition domain binding leads to much greater avidity. The levels of MBL in human serum vary greatly between individuals (15), from <50 ng/ml to >10 μg/ml.

MBL has a structure and function similar to those of the complement protein C1q and participates in the host defense

* The MALDI mass spectrometer used in this work was purchased with a grant from the Biotechnology and Biological Sciences Research Council. The costs of publication of this article were defrayed in part by the payment of page charges. This article must therefore be hereby marked "*advertisement*" in accordance with 18 U.S.C. Section 1734 solely to indicate this fact.

¶ To whom correspondence should be addressed. Tel.: 44-1865-275-352; Fax: 44-1865-275-729; E-mail: bob.sim@bioch.ox.ac.uk.

[1] The abbreviations used are: MBL, mannan-binding lectin; MASP, MBL-associated serine protease; PBS, phosphate-buffered saline; ELISA, enzyme-linked immunosorbent assay; TNP, 2,4,6-trinitrophenyl; BSA, bovine serum albumin; Tricine, *N*-[2-hydroxy-1,1-bis(hydroxymethyl)ethyl]glycine; MES, 4-morpholineethanesulfonic acid; 2-AB, 2-aminobenzamide; NP, normal phase; HPLC, high pressure liquid chromatography; MALDI-TOF, matrix-assisted laser desorption ionization time-of-flight; CHES, 2-(cyclohexylamino)ethanesulfonic acid; BisTris, 2-[bis(2-hydroxyethyl)amino]-2-(hydroxymethyl)propane-1,3-diol; CH, constant heavy.

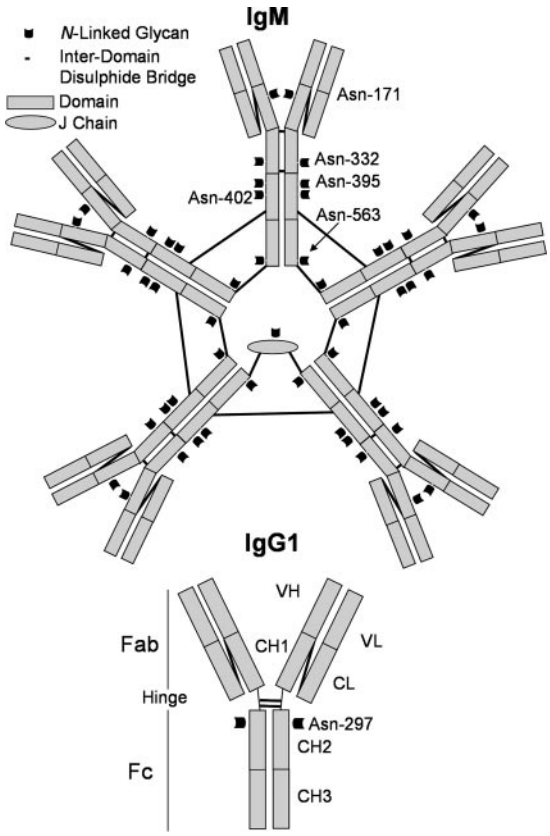

FIG. 1. **Diagrammatic structure of pentameric IgM and IgG1.** The diagrammatic representation of pentameric IgM and IgG1 shows the variable and constant heavy chain (*VH* and *CH*, respectively) and light chain (*VL* and *CL*, respectively) domains. The diagram also shows the Fab and Fc domains. The locations of the asparagines to which *N*-linked glycans are attached are marked. The J chain is also shown on the IgM structure.

response through two major pathways. First, it acts directly as an opsonin, promoting phagocytosis of foreign material to which it has bound. Second, it triggers the lectin pathway of complement activation (18, 19). MBL circulates bound to MBL-associated serine proteases (MASPs) (19). Three MASPs have been characterized to date: MASP-1 and MASP-2 (20, 21) and MASP-3 (22). MASP-2 has been shown to cleave complement components C4 and C2, resulting in the formation of the C3 convertase C4b2a. The biological roles of MASP-1 and MASP-3 are unknown, although MASP-1 is known to cleave fibrinogen and activate Factor XIII (19).

Glycoproteins, including the immunoglobulins, consist of a collection of glycosylated variants (glycoforms) in which a single amino acid sequence is diversified by the variable processing of glycans at each of the glycosylation sites. Some of these subpopulations may have glycans that are ligands for MBL. This has been demonstrated for IgG. MBL has been shown to bind agalactosyl glycoforms of IgG (known as IgG-G0) in which the single Asn-297 *N*-linked site in the IgG γ chain is occupied by glycans that have terminal GlcNAc residues (23). IgG-G0 accounts for ~35% of normal serum IgG (24). MBL also binds polymeric forms of serum IgA (25), but the IgA glycans to which MBL binds have not been identified.

There are conflicting reports about whether MBL interacts with IgM. Immobilized human myeloma IgM does not bind to human MBL (26), although mouse IgM and, to a lesser extent, human and bovine IgM can bind to immobilized rabbit MBL (27). Rat MBL has also been reported to bind human IgM (28). The oligomannose structures that occupy Asn-402 and Asn-563 are potential ligands for MBL binding (28).

Electron microscopy studies have shown that a considerable conformational change occurs in the IgM pentamer when it has bound to antigen. This might allow IgM to expose its oligomannose glycans upon antigen binding, providing a potential mechanism of clearance of IgM after its initial recognition via an MBL-dependent pathway (3). IgM interacts efficiently with the complement system and constitutes a first line of defense against infection. However, hexameric IgM is 20 times more efficient at activating complement compared with pentameric IgM (1, 29, 30). The complement activation by IgM is attributed to C1q binding. The charged residues Asp-417, Glu-418, and His-420 in the Cμ3 domain of IgM have been proposed as the binding site for C1q on IgM (31).

Here, we present the first comprehensive report of normal human serum IgM glycosylation and identify glycoforms of human serum IgM that do bind to MBL. Using molecular modeling, we have constructed a complete structure of glycosylated pentameric IgM and have assessed the accessibility of the identified oligomannose structures as binding targets for MBL.

EXPERIMENTAL PROCEDURES

Antibodies and Antisera—Rabbit antiserum against recombinant MBL was adsorbed to remove anti-mannan antibodies and rheumatoid factors as described previously (32).

Protein Concentration—Protein samples (25 μg in any volume) were concentrated for general SDS-PAGE analysis by incubation with slow rotation at room temperature for 30 min with a 5-μl packed volume of StrataClean™ resin (Stratagene, Zuidoost, The Netherlands). The samples were then spun at 13,000 rpm for 1 min, and the supernatant was discarded. The resin was resuspended in 20 μl of SDS-PAGE sample buffer (200 mM Tris, 8 M urea, 2% SDS, and 1 mM EDTA, pH 8) and loaded onto the gel.

IgM was concentrated by chloroform/methanol precipitation adapted from the procedure described previously (33). To 100 μl of IgM sample (in phosphate-buffered saline (PBS) and 0.5 mM EDTA) was added 400 μl of methanol. This was vortexed and spun at 13,000 rpm for 30 s, and 100 μl of chloroform was added, vortexed, and spun again. To this was added 300 μl of water, followed by vortexing and spinning. There was a phase separation; the upper phase was removed and discarded; and 300 μl of methanol was added and vortexed. The precipitated IgM was pelleted by spinning at 13,000 rpm for 3 min. The supernatant was removed and discarded, and the pellet was dried in a vacuum centrifuge (Savant SpeedVac®, Thermo LifeSciences, Basingstoke, UK) for 30 min. This pellet was dissolved in 30 μl of sample buffer for SDS-PAGE analysis.

Large-scale IgM Purification from Human Serum—The purification method was adapted from that of Johnstone and Thorpe (34). 1 liter of citrated pooled normal human plasma (HDS Supplies, High Wycombe, UK) was made 20 mM $CaCl_2$ and left overnight at 4 °C to clot. The clot was filtered through muslin. IgM was precipitated from the serum at low salt by dialysis against 3 × 10 liters of 2 mM sodium phosphate, pH 6.0. The sample was centrifuged at 11,000 × *g* for 20 min at 4 °C; the supernatant was discarded; and the pellet washed twice by resuspension in 100 ml of 2 mM sodium phosphate, pH 6.0, at 4 °C. The pellet was redissolved in 100 ml of Tris-buffered saline (10 mM Tris-HCl, 150 mM NaCl, and 0.5 mM EDTA, pH 7.3) at room temperature and centrifuged at 11,000 × *g* for 20 min at room temperature to remove undissolved material. A 50-ml sample was then applied to a Sepharose 4B gel filtration column (2.6 × 100 cm; Amersham Biosciences AB, Uppsala, Sweden) pre-equilibrated with Tris-buffered saline, pH 7.4, at 4 °C, and the fractions judged to contain IgM by SDS-PAGE analysis were pooled. The sample was run through 215 ml of Matrex Blue B resin (3.2 × 30 cm; Amicon Inc., Beverly, MA) pre-equilibrated with Tris-buffered saline, pH 7.4. The flow-through fractions containing IgM were collected and pooled. IgM still contained small amounts of IgG and IgA identified by SDS-PAGE analysis and direct enzyme-linked immunosorbent assay (ELISA) using alkaline phosphatase-conjugated goat anti-human IgG (γ chain-specific; A3187, Sigma, Poole, UK) and alkaline phosphatase-conjugated goat anti-human IgA (α chain-specific; Sigma). IgG was removed using a 5-ml HiTrap-protein G column (Amersham Biosciences AB), and IgA was removed by passage through an anti-IgA (α chain-specific)-Sepharose column (A2691, Sigma). The final IgM was judged by SDS-PAGE analysis to be >95% pure and was dialyzed against

Dulbecco's PBS (8.2 mM Na_2HPO_4, 1.5 mM KH_2PO_4, 139 mM NaCl, and 3 mM KCl, pH 7.4; Oxoid Ltd., Hampshire, UK) containing 0.5 mM EDTA.

Small-scale IgM Purification from Human Serum Using an ImmunoPure® IgM Purification Kit—The ImmunoPure® IgM purification kit was purchased from Pierce. The column was rabbit MBL-conjugated to a 4% beaded agarose support (5 ml), sold as a kit for purification of mouse IgM from ascites fluid. The column was run using human serum according to the directions of the manufacturer. The column was prewashed with 5 ml of ImmunoPure® MBP (mannan-binding protein) column preparation buffer (Tris, sodium chloride, sodium azide, and EDTA, pH 7.4) at room temperature and then equilibrated with 20 ml of ImmunoPure® IgM binding buffer (Tris, sodium chloride, calcium chloride, and sodium azide, pH 7.4) at 4 °C. Human serum (500 μl) from citrated plasma as described above diluted 1:1 with ImmunoPure® IgM binding buffer was applied to the column at 4 °C and allowed to enter the resin completely. An additional 500 μl of ImmunoPure® IgM binding buffer was added and also allowed to enter the resin. The column was then incubated at 4 °C for 30 min and washed with 42 ml of ImmunoPure® IgM binding buffer. Bound protein was eluted at room temperature with 8 ml of ImmunoPure® IgM elution buffer (Tris, sodium chloride, sodium azide, and EDTA, pH 7.4).

The bound proteins were analyzed by SDS-PAGE and found to be a complex mixture containing <5% IgM. The material in the buffer as described above was run on a 10-ml anti-human IgM-agarose column (Medical Research Council Immunochemistry Unit), and the column was washed with 10 mM Hepes, 1 M NaCl, and 0.5 mM EDTA, pH 7.4. IgM was eluted from the column with 3 M $MgCl_2$, and 1-ml fractions were collected. The fractions containing protein (detected by reading the absorbance at 280 nm) were pooled and dialyzed against 10 mM Hepes, 1 M NaCl, and 0.5 mM EDTA, pH 7.4. The material was passed through a 1-ml HiTrap-protein G column (Amersham Biosciences AB) to remove IgG. IgM was judged to be >95% pure by SDS-PAGE analysis.

Preparation of 2,4,6-Trinitrophenyl (TNP)-conjugated Bovine Serum Albumin (BSA) and TNP-BSA-Sepharose—TNP-BSA was prepared by mixing 10 ml of 1% BSA in PBS and 0.5 mM EDTA with 2 ml of 5% (w/v) picrylsulfonic acid solution (P2297, Sigma). The pH was monitored to keep the mixture neutral to prevent BSA precipitation, and the mixture was left for 4 h at room temperature. TNP-BSA was then dialyzed exhaustively at 4 °C against PBS and 0.5 mM EDTA. TNP-BSA-Sepharose was prepared with 2 g of cyanogen bromide-activated Sepharose 4B (Amersham Biosciences AB) according to the manufacturer's instructions. Excess binding sites on the resin were blocked with 100 mM ethanolamine HCl and 150 mM NaCl, pH 8.5, and mixed by rotating for 2 h at room temperature. The resin was then equilibrated with PBS and 0.5 mM EDTA. The final resin contained 5 mg of TNP-BSA/ml of packed Sepharose.

Purification and Arthrobacter ureafaciens Sialidase (ABS)/Bovine Testis β-Galactosidase (BTG) Treatment of Anti-TNP-BSA IgM from Human Serum—IgM was low salt-precipitated from 1 liter of pooled human serum (citrated pooled normal human plasma from HDS Supplies) and redissolved as described above. The IgM solution in Tris-buffered saline was spun at 60,000 rpm for 45 min to diminish lipid contamination, which formed as a layer at the meniscus. The material was passed through 5 ml of TNP-BSA-Sepharose in PBS and 0.5 mM EDTA. Bound material was eluted using 0.2 M glycine HCl, pH 2.2, and dialyzed against PBS and 0.5 mM EDTA. The major proteins eluted were IgM, IgG, Factor H, and IgA (identified by SDS-PAGE and mass spectrometry) (data not shown). IgG and IgA were removed as described above. Factor H was removed from the preparation by running the material through a 10-ml MRC OX23-Sepharose column (35). The final preparation was judged to be >95% pure IgM by SDS-PAGE analysis. The preparation was then treated with the exoglycosidases ABS (EC 3.2.1.18) at 3 milliunits/ml and BTG (EC 3.2.1.23) at 1 unit/ml to cleave the complex glycans on IgM to a terminal GlcNAc (a residue that would bind MBL). anti-TNP-BSA IgM (4.8 μg) in 4 ml of PBS was incubated with 30 microunits of ABS and 20 milliunits of BTG for 16 h at 37 °C and for several days at 4 °C.

IgM Quantification by ELISA—The wells of an ELISA plate (Maxisorp, Nunc, Roskilde, Denmark) were coated with 100 μl of 10 μg/ml goat anti-human IgM (μ chain-specific; H15000, Caltag Laboratories, Burlingame, CA) in 0.1 M $NaHCO_2$, pH 9.5. The wells were incubated overnight at 4 °C; blocked with 400 μl of PBS and 0.1% Tween 20 for 2 h at room temperature; and washed three times with 200 μl of PBS, 0.1% Tween 20, and 0.5 mM EDTA. IgM preparations were serially diluted in PBS and 0.1% Tween 20. IgM from the large-scale preparation was quantified from absorbance readings at 280 nm (extinction coefficient of 1.18 for 1 mg/ml) (34) and incubated, as a standard, for 1 h at room temperature. The wells were washed three times with PBS and 0.1% Tween 20, incubated with alkaline phosphatase-conjugated goat anti-human IgM (μ chain-specific; 1:2000 dilution; A3437, Sigma) for 1 h at room temperature, and washed again. 100 μl of *p*-nitrophenyl phosphate substrate (N1891, Sigma) was added; and the absorbance was read at 405 nm after 30 min.

SDS-PAGE Separation of the J Chain and Western Blotting for the J Chain—The J chain has an apparent molecular mass similar to that of the Ig light chain on SDS-polyacrylamide gel. To separate these proteins for analysis of *N*-linked glycans, 20 μg of pooled normal human IgM was run on a Tricine-10–20% acrylamide gradient precast gel (Invitrogen, Paisley, UK) for 70 min at 150 V in 1× NuPAGE® MES SDS running buffer (NP0002, Invitrogen). These gels were stained with SimplyBlue SafeStain (LC3065, Invitrogen) for 30 min and destained in water to visualize the bands.

Western blotting was performed to locate the position of the J chain on the gel. An unstained gel was soaked in Western transfer buffer (25 mM Tris, 0.2 M glycine, and 20% (v/v) methanol) for 10 min. A transfer membrane (Millipore Corp., Bedford, MA) was prepared by soaking for 10 s in methanol, for 15 min in water, and for 15 min in transfer buffer. The semidry blot was run at 1.2 mA/cm^2 for 1 h at room temperature. The membrane was blocked with 1% (w/v) milk solution for 2 h at room temperature, washed three times for 5 min each with PBS and 0.1% Tween 20, and then incubated for 1 h with 0.5 μg/ml mouse anti-human J chain antibody (MCA693, Serotec, Oxford, UK) in the wash buffer. The membrane was washed three times, incubated with alkaline phosphatase-conjugated goat anti-mouse IgG (γ chain-specific; 1:2000 dilution; A3438, Sigma) for 1 h at room temperature, washed three times, and visualized using Sigma FAST™ 5-bromo-4-chloro-3-indolyl phosphate/nitro blue tetrazolium tablets (B5655, Sigma). This identified the position of the J chain that was separated the light chain.

Removal of N-Linked Glycans for Analysis—Human IgM (20 μg) prepared by the large-scale method or by small-scale method using an ImmunoPure® IgM purification kit was run on SDS-polyacrylamide gel, followed by in-gel *N*-linked glycan release using peptide *N*-glycanase F (1000 units/ml; glycopeptidase, EC 3.5.1.52) as described previously (36, 37).

2-Aminobenzamide (2-AB) Labeling—Released glycans were labeled by reductive amination with the fluorophore 2-AB (38) using a LudgerTag™ 2-AB glycan labeling kit (Ludger Ltd., Oxford, UK).

Normal Phase (NP) HPLC and Weak Anion Exchange HPLC—Labeled glycans were separated by NP-HPLC (39) and weak anion exchange HPLC (40). Glycan profiles from NP-HPLC were calibrated against a dextran ladder prepared from hydrolyzed and 2-AB-labeled glucose oligomers (39). Glycans were assigned glucose units, and glycan structure/composition was predicted by reference to a glycan data base using the program PeakTime.[2]

Exoglycosidase Digestions—Exoglycosidases were used to confirm the structures of glycans present in the preparations in conjunction with NP-HPLC (37). Enzymes were used at the concentrations recommended by the manufacturers, and digestions were carried out using 50 mM sodium acetate buffer, pH 5.5, for 16 h at 37 °C. The following enzymes were supplied by Glyko Inc. (Upper Heyford, UK): ABS (1–2 units/ml), almond meal α-fucosidase (3 milliunits/ml; EC 3.2.1.51), BTG (1 unit/ml), jack bean α-mannosidase (100 milliunits/ml; EC 3.2.1.24), *Streptococcus pneumoniae* β-*N*-acetylhexosaminidase (120 units/ml; EC 3.2.1.52), and bovine kidney fucosidase (100 units/ml; EC 3.1.1.51). Europa Bioproducts (Cambridge, UK) supplied *S. penumoniae* recombinant sialidase expressed in *E. coli* (1 unit/ml; Nanl; EC 3.2.1.18). The glucosidase II was prepared in the Glycobiology Institute.

Mass Spectrometry—Non-2-AB-labeled *N*-linked glycans were analyzed by MALDI-TOF mass spectrometry from 2,5-dihydroxybenzoic acid (41).

Calculations of the Number of GlcNAc-terminating and Hybrid Glycans/IgM Pentamer—The average number of GlcNAc-terminating and hybrid structures/IgM pentamer was calculated to identify the number of potential MBL ligands present on each IgM pentamer. For example, taking values from Table III, pooled human IgM had a total of 7.5% structures that could potentially act as ligands for MBL occupying Asn-171, Asn-332, and Asn-395, with a probability of 0.075 at each site. There are 10 μ chains/IgM pentamer, each with the three *N*-linked glycosylation sites (Asn-171, Asn-332, and Asn-395) bearing complex sugars; therefore, 2.3 (*i.e.* 30 × 0.075) GlcNAc-terminating/hybrid glycans are present, on average, on each IgM pentamer.

[2] E. Hart, R. A. Dwek, and P. M. Rudd, unpublished data.

MBL Purification—The purification procedure has been described previously (32, 42). Trace contaminants (IgG and IgM) were identified by SDS-PAGE analysis and direct ELISA using alkaline phosphatase-conjugated goat anti-human IgG (γ chain-specific) and alkaline phosphatase-conjugated goat anti-human IgM (μ chain-specific). The preparation was passed through a 1-ml HiTrap-protein G column and then 10 ml of anti-human IgM-agarose. The protein was dialyzed against 10 mM Hepes, 149 mM NaCl, and 5 mM $CaCl_2$, pH 7.4; concentrated by binding to 500 μl of mannose-agarose (M6400, Sigma); and eluted with 10 mM Hepes, 140 mM NaCl, and 5 mM EDTA, pH 7.4. The sample was judged to be >95% pure by SDS-PAGE analysis. The concentration of MBL was calculated using a mannan capture MBL ELISA (32).

Assay for MBL Binding to IgM Preparations—The procedure for ELISA was that described by Arnold *et al.* (32). The wells of an ELISA plate were coated with 100 μl of 50 μg/ml TNP-BSA and blocked by the same method described for the IgM ELISA. After blocking, the wells were incubated with 100 μl of ABS- and BTG-treated anti-TNP-BSA IgM (120 ng/well) in PBS (previously shown by ELISA to saturate the TNP-BSA (data not shown)). In other wells, ABS- and BTG-treated anti-TNP-BSA IgM (120 ng/well), IgM from the large-scale bulk-purified serum IgM (120 ng/well), or IgM purified from the MBL-conjugated resin (120 ng/well) was coated directly onto the wells. Mannan (M7504, Sigma) and BSA were used for coating as positive and negative controls, respectively, at 50 μg/ml. An additional negative control of the enzyme digestion mixture of ABS and BTG was bound directly to the well without anti-TNP-BSA IgM. MBL binding was assessed using a 1:700 dilution of rabbit anti-human polyclonal MBL antiserum and a 1:2000 dilution of alkaline phosphatase-conjugated anti-rabbit monoclonal IgG (γ chain-specific, RG-96; A2556, Sigma) as described by Arnold *et al.* (32) and developed with the substrate 1 mM 4-methylumbelliferyl phosphate (474431, Calbiochem) in 5 mM CHES and 1 mM $MgCl_2$, pH 9.8, and the fluorescence was measured at λ_{ex} = 355 nm and λ_{em} = 460 nm after 1 h.

Molecular Modeling—Sequence alignment was performed using Align (43) on the equivalent domains of IgG and IgE (Swiss-Prot accession numbers P01857 and P01854, respectively). Molecular modeling was performed on a Silicon Graphics Fuel workstation using Insight II and Discover software (Accelrys Software Inc., San Diego, CA). Crystal structures used as the basis for modeling were obtained from the Protein Data Bank (44). The monomeric IgM molecular models for the Fc and hinge domains were based on the crystal structure of the IgE Fc domain (45), and the Fab domains were based on the crystal structure of IgG (46). The J chain was based on the J chain from the molecular model of secretory IgA (47). *N*-Glycan structures were generated using the data base of glycosidic linkage conformations (48, 49) and *in vacuo* energy minimization to relieve unfavorable steric interactions. The Asn-GlcNAc linkage conformations were based on the observed range of crystallographic values (50). The details of the construction of the IgM pentamer from the monomer units will be published elsewhere.[3]

RESULTS

IgM Quantification from Purified IgM Preparations—The pooled serum for the IgM purifications contained 1774 μg of IgM/ml of serum. Large-scale IgM bulk-purified from 1 liter of pooled serum (Fig. 2*a*) gave a final yield of 78 μg of IgM/ml of serum (4% of total IgM), which was quantified by reading the absorbance at 280 nm.

The MBL column from the ImmunoPure® IgM purification kit had a binding capacity of ~180 μg of human IgM. Repeated passage of 0.5 ml of serum over the column indicated that ~200 μg of IgM could be extracted from 0.5 ml of serum (~22% of total IgM). Bound IgM that eluted with EDTA was impure, representing ~5% of the eluted proteins. When further purified using a protein G resin to remove IgG and an anti-IgM resin to select IgM (Fig. 2*b*), the final yield of IgM was 68 μg from 0.5 ml of serum (*i.e.* 8% of total IgM). Anti-TNP-BSA IgM was derived from 1 liter of pooled human serum (Fig. 2*c*) with a yield of 0.042 μg of anti-TNP-BSA IgM/ml of serum.

N-Linked Glycans of Pooled Human Serum IgM—Glycans were released from the μ chain of IgM prepared by large-scale purification (Fig. 2*a*). The released glycans were analyzed by MALDI-TOF mass spectrometry and NP-HPLC of the 2-AB-labeled material (Fig. 3). Structures of the glycans were assigned based on their glucose units, shifts in glucose units with enzyme digest arrays, and molecular masses (Table I). Sialylated glycans could be digested with ABS, but not with Nan1, indicating that all sialic acid residues are α2,6 (not α2,3)-linked to galactose. Weak anion exchange HPLC and enzyme digestions showed the presence of neutral and mono- and disialylated structures as well as oligomannose glycans.

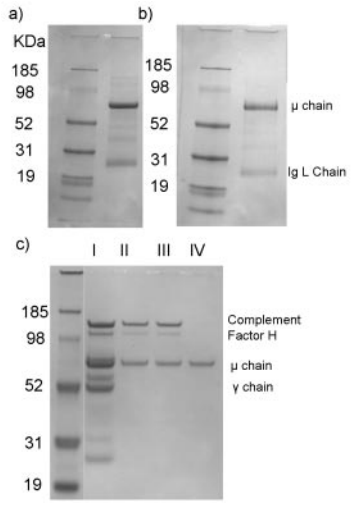

FIG. 2. **SDS-PAGE analysis of reduced and alkylated IgM.** Samples were run on 4–15% BisTris gels (Invitrogen) alongside 7 μl of MultiMark protein ladder (Invitrogen). *a*, 20 μg of the purified IgM preparation from normal human serum. *b*, 20 μg of purified IgM eluted from the MBL resin after the additional purification steps with anti-human IgM-agarose and HiTrap-protein G. Bands were excised and analyzed. *c*, purification of anti-TNP-BSA IgM. *Lane I*, material eluted from TNP-BSA-Sepharose; *lane II*, material after the HiTrap-protein G resin; *lane III*, material after the anti-human IgA resin; *lane IV*, final material after the OX23 resin. The presence of IgM was confirmed using a direct ELISA with alkaline phosphatase-conjugated goat anti-human IgM (μ chain-specific). *Ig L Chain*, Ig light chain.

N-Linked Glycosylation of Asn-402 and Asn-563—Normal human serum IgM contains $GlcNAc_2Man_{5-9}$ structures (Table I), with two predominant oligomannose structures, $GlcNAc_2Man_6$ and $GlcNAc_2Man_8$, which account for 9.5 and 4.1% of the total glycan pool, respectively. This is consistent with previous myeloma IgM glycan analysis (3, 11–12). Assuming full occupancy of all five glycosylation sites and that Asn-402 and Asn-563 contain only oligomannose glycans, then oligomannose glycans should compose 40% of the total glycan pool. In fact, oligomannose glycans composed only 23.4% of the *N*-linked glycan pool in this pooled normal human serum IgM. The Asn-402 site in the IgM Fc domain is homologous to the Asn-297 *N*-linked glycosylation site in IgG, Asn-354 in IgD, and Asn-394 in IgE, which are all fully occupied (32). Asn-563 has been shown to have a 75% occupancy in human-mouse hybridoma human IgM (51) and a 44% occupancy in murine IgM (52). Assuming 100% occupancy of Asn-402, 23.4% oligomannose glycans would account for 17% occupancy at Asn-563.

IgE and IgM possess a CH2 hinge domain, replacing the flexible hinge region in IgG, IgD, and IgA. The crystal structure of IgE (45) showed that the CH2 hinge domain adopts an asymmetrically bent conformation relative to the Fc domain. The relatively unprocessed glycans on the IgE Fc domain Asn-394 *N*-linked glycosylation site remain predominantly $GlcNAc_2Man_5$ and $GlcNAc_2Man_6$ structures. This can be explained by the CH2 hinge domain blocking access to the glycans and thus preventing processing. The CH2 domain must then "flip" between two bent quaternary conformations to block access to the two Asn-394 glycans on opposite sides of the Fc

[3] J. N. Arnold, unpublished data.

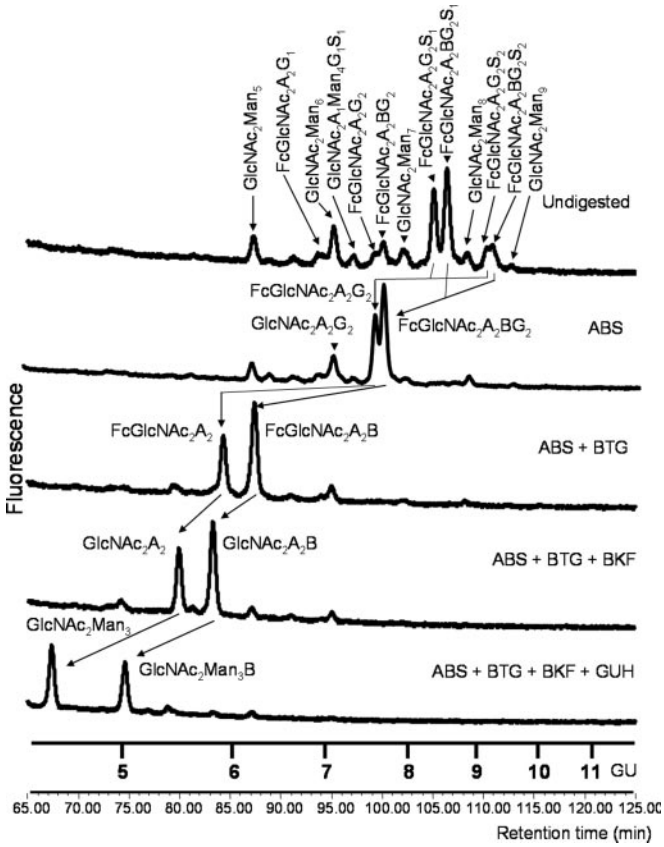

FIG. 3. **NP-HPLC exoglycosidase digestion profile of the glycan pool from IgM.** 2-AB-labeled *N*-linked glycans were digested by exoglycosidases and analyzed by NP-HPLC. All *N*-glycans have two core GlcNAc residues. *Fc*, core fucose linked α1–6 to the inner GlcNAc residue; Man_n, number (n) of mannose residues on core GlcNAc residues: A_n, number of antennae on the trimannosyl core (A_2 = biantennary); *B*, bisecting GlcNAc linked β1–4 to the inner mannose; G_n, number of galactose residues on the antennae; S_n, number of sialic acids on the antennae. Percentage areas and glucose units (*GU*) are shown in Table I. The exoglycosidases used were ABS (removes sialic acid), BTG (removes galactose), bovine kidney fucosidase (*BKF*; removes core fucose), and *N*-acetyl-β-glucosaminidase (*GuH*; removes terminal GlcNAc).

TABLE I
Pooled normal IgM μ chain N-linked glycans
GU, glucose units.

Structure[a]	GU	Molecular mass[b]	Composition[c]				Glycan pool
			Hex	HexNAc	Fuc	Neu5Ac	
		Da					%
$GlcNAc_2A_1$	4.90	ND	3	3	0	0	0.9
$GlcNAc_2A_2$	5.03	1339.4	3	4	0	0	0.4
$GlcNAc_2A_2B$	5.58	ND	3	5	0	0	1.3
$FcGlcNAc_2A_2$	5.71	1485.5	3	4	1	0	0.2
$GlcNAc_2A_3$	5.71	ND	3	5	0	0	0.2
$FcGlcNAc_2A_2B$	5.90	ND	3	5	1	0	0.2
$GlcNAc_2Man_5$	6.17	1257.4	5	2	0	0	5.6
$GlcNAc_2A_1Man_4G_1$	6.33	1460.6	5	3	0	0	0.7
$GlcNAc_2A_2G_1$	6.60	1501.5	4	4	0	0	1.1
$GlcNAc_2A_2BG_1$	6.60	1704.6	4	5	0	0	0.7
$FcGlcNAc_2A_2G_1$	6.87	1647.6	4	4	1	0	0.4
$FcGlcNAc_2A_2BG_1$	6.87	1850.6	4	5	1	0	0.6
$GlcNAc_2A_3G_1$	6.87	1704.6	4	5	0	0	2.1
$GlcNAc_2Man_6$	7.06	1419.4	6	2	0	0	9.5
$GlcNAc_2A_2G_2$	7.06	1663.6	5	4	0	0	ND
$GlcNAc_2A_2BG_2$	7.30	1886.7	5	5	0	0	ND
$GlcNAc_2A_1Man_4G_1S_1$	7.30	DS	5	3	0	1	1.9
$FcGlcNAc_2A_2G_2$	7.58	1809.6	5	4	1	0	1.1
$GlcNAc_2A_3G_2$	7.58	1866.7	5	5	0	0	
$FcGlcNAc_2A_2G_1S_1$	7.58	DS	4	4	1	1	1.8
$FcGlcNAc_2A_2BG_2$	7.66	2012.8	5	5	1	0	4.2
$FcGlcNAc_2A_2BG_1S_1$	7.66	DS	4	5	1	1	1.1
$FcGlcNAc_2A_3G_2$	7.76	2012.8	5	5	1	0	1.0
$GlcNAc_2Man_7$	7.92	1581.6	7	2	0	0	3.2
$GlcNAc_2A_2G_2S_1$	7.92	DS	5	4	0	1	1.7
$GlcNAc_2A_2BG_2S_1$	8.22	DS	5	5	0	1	1.1
$FcGlcNAc_2A_2G_2S_1$	8.33	DS	5	4	1	1	18.7
$FcGlcNAc_2A_2BG_2S_1$	8.52	2325.8	5	5	1	1	26.2
$GlcNAc_2Man_8$	8.81	1743.6	8	2	0	0	4.1
$FcGlcNAc_2A_2G_2S_2$	9.11	DS	5	4	1	2	2.6
$FcGlcNAc_2A_3G_2S_1$	9.11	2325.8	5	5	1	1	1.9
$FcGlcNAc_2A_2BG_2S_2$	9.19	DS	5	5	1	2	4.8
$GlcNAc_2Man_9$	9.51	1905.7	9	2	0	0	1.0

[a] Glycan nomenclature is explained in the legend to Fig. 3.
[b] Molecular masses are of unlabeled glycans, detected as $[M + Na]^+$ by MALDI mass spectrometry. All masses were within 0.2 mass units of calculated values. DS, desialylated mass detected. Sialylated structures during MALDI lost most sialic acid residues. ND, not detected by NP-HPLC.
[c] Compositions were deduced from mass values.

domain (32). The extent of processing at the Asn-402 site in IgM is similar to that at Asn-394 in IgE. The CH2 hinge domain in IgM may also adopt this asymmetrically bent conformation and thus lead to similar processing of the glycans occupying Asn-402 as observed in IgE.

N-Linked Glycosylation of Asn-171, Asn-332, and Asn-395—The non-oligomannose complex structures accounted for 76.6% of the released glycan pool and must be found chiefly at Asn-171, Asn-332, and Asn-395. Monosialylated structures accounted for 70.9% and disialylated structures for 9.7% of the complex glycan pool (Table I). Bisected structures (those containing "B" in Table I) accounted for 52.5% of the complex glycan pool. Fukuta *et al.* (53) found comparable quantities of bisected glycans in transformed B cell line human IgM (named IgM-12; 49.9, 67.8, and 81.3% at each site, respectively); however, human-mouse hybridoma IgM3-4 has significantly fewer bisected structures (3.7, 8.7, and 15.3% at each site, respectively). In this study, core-fucosylated structures ("Fc" in Table I) accounted for 84.5% of the complex glycan pool of normal human serum IgM, comparable with the results for both myelomas IgM3-4 and IgM-12 (53).

In heterohybridoma human IgM (54), hybrid structures $GlcNAc_2A_1Man_4G_1$ and $GlcNAc_2A_1Man_4G_1S_1$ (see the legend to Fig. 3 for explanation of glycan nomenclature) have one arm terminating in mannose, occur at Asn-171, and account for 42.5% of the glycans at that site. However, the human serum IgM studied here contained a significantly lower percentage of hybrid structures (0.9% of $GlcNAc_2A_1Man_4G_1$ and 2.5% of $GlcNAc_2A_1Man_4G_1S_1$) (Fig. 3).

N-Linked Glycans of the Pooled IgM J Chain—The J chain of IgM has a single *N*-linked glycosylation site. The *N*-linked glycans were released from the pooled serum IgM J chain, 2-AB-labeled, and analyzed by NP-HPLC before and after digestion with ABS and with ABS and BTG (Fig. 4 and Table II). Structural assignments were made based on glucose units and exoglycosidase digestions. The profile shows the presence of neutral and mono- and disialylated structures (Fig. 4). The normal human IgM J chain was found to be occupied predominantly by $GlcNAc_2A_2G_2S_1$ structures, accounting for 44% of the glycan pool. This structure is also the most abundant glycan in the secretory IgA J chain (45). Royle *et al.* (47) also identified a comparable content of $FcGlcNAc_2A_2G_2S_1$ (13.6%), $GlcNAc_2A_2G_2S_2$ (13.8%), and $FcGlcNAc_2A_2G_2S_2$ (17%). Here, we report 15, 17, and 8% of these three structures, respectively, on the IgM J chain. Normal human serum IgM J chain glycans were found to be 25.7% core-fucosylated and to have no bisecting GlcNAc residues.

Comparison of the Glycans in Pooled Serum IgM and Those in IgM Eluted from the MBL Resin—The *N*-linked glycans were released from the purified IgM μ chain eluted from the MBL-conjugated resin (Fig. 2*b*) and subjected to NP-HPLC, and

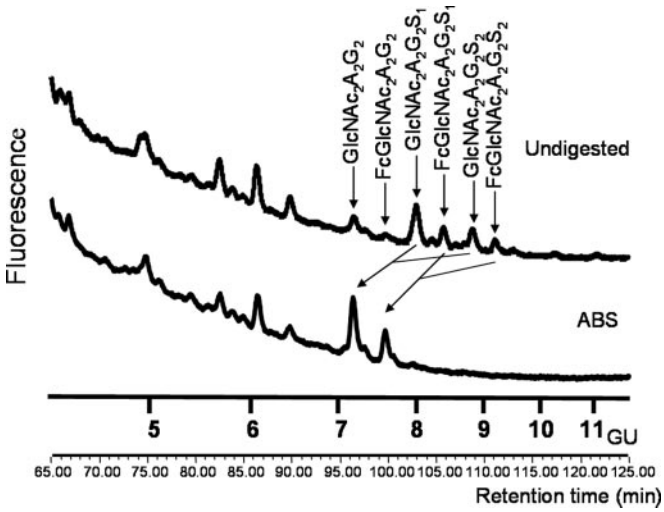

FIG. 4. **NP-HPLC exoglycosidase digestion of glycan pool of pooled normal IgM J chain.** The *N*-linked glycans of the IgM J chain were analyzed by NP-HPLC before and after sialidase digestion. Percentage areas and glucose units (*GU*) are shown in Table II. All unlabeled peaks are not glycans.

TABLE II
Pooled normal IgM J chain N-linked glycans
See Table I for details. GU, glucose units.

Structure	GU	Glycan pool
		%
$GlcNAc_2A_2G_2$	7.12	12.5
$FcGlcNAc_2A_2G_2$	7.54	2.7
$GlcNAc_2A_2G_2S_1$	7.95	44
$FcGlcNAc_2A_2G_2S_1$	8.34	15
$GlcNAc_2A_2G_2S_2$	8.78	17
$FcGlcNAc_2A_2G_2S_2$	9.14	8

glycan structures were assigned to the peaks. The same glycan structures were identified in both IgM preparations (Fig. 5), but there was a 97.3% increase in GlcNAc-terminating and hybrid structures (Table III, part A) in IgM eluted from the MBL resin. These structures occupied Asn-171, Asn-332, and Asn-395, as Asn-402 and Asn-563 are occupied only by oligomannose structures. There was also a 7.8% increase in overall oligomannose structures (Table III, part B) from the total glycan pool, mostly by an increase in $GlcNAc_2Man_8$ structures.

MBL Binding Studies—The binding of MBL to the purified IgM preparations was assessed using microtiter plates that had been coated with antigen-bound IgM or directly immobilized IgM (Fig. 6). Assays were carried out in triplicate or over 6 wells with additional negative EDTA controls. Only slight binding to antigen-bound IgM (ABS- and BTG-treated anti-TNP-BSA IgM) and bulk serum IgM was observed. However, directly immobilized IgM eluted from the MBL resin, and directly immobilized ABS- and BTG-treated anti-TNP-BSA IgM showed a much higher level of MBL binding. The ABS and BTG enzyme mixture alone showed no MBL binding.

DISCUSSION

N-Linked Glycosylation of Normal Human Serum IgM—IgM contains a range of *N*-linked glycans (Table I) terminating predominantly in sialic acid and galactose, but also in mannose and GlcNAc (Fig. 7). By reference to previous reports (3, 6, 12), we conclude that oligomannose glycans are confined to Asn-402 and Asn-563. The glycosylation sites Asn-171, Asn-332, and Asn-395 are likely to be occupied by complex glycans. The glycans at these sites terminated predominantly in galactose or sialic acid (95.1%), and a small population (4.9%) terminated in

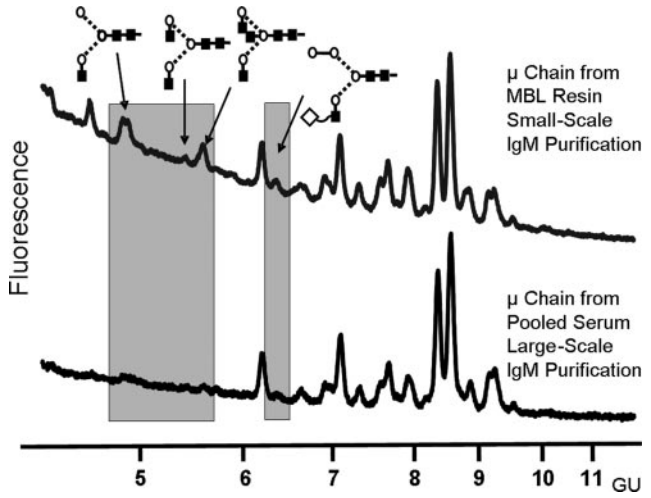

FIG. 5. **Comparison of the NP-HPLC glycan profiles of normal human IgM and the glycans of IgM eluted from the MBL resin.** The two undigested NP-HPLC profiles are similar. There is a significant enrichment (*highlighted*) of *N*-linked glycans that terminate in sugars that could potentially act as ligands for MBL (either mannose or GlcNAc). ■, GlcNAc; ◇, galactose; ——, β linkage; ····, α linkage; *curved line*, 1–6 linkage; –, 1–4 linkage; |, 1–2 linkage.

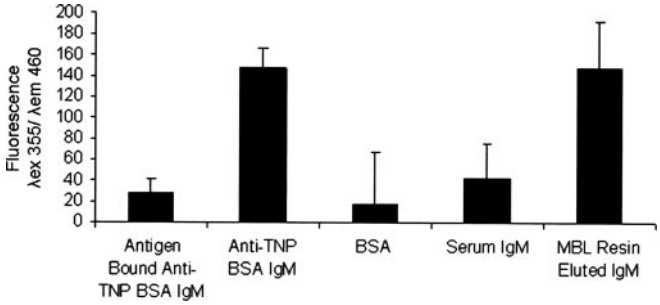

FIG. 6. **MBL binding to IgM preparations.** Microtiter plate wells were coated with TNP-BSA (50 μg/well), blocked, and subsequently saturated with ABS- and BTG-treated anti-TNP-BSA IgM (120 ng/well). The ABS and BTG treatment cleaves all complex glycans to a terminal GlcNAc residue to maximize the number of MBL-binding glycan targets. ABS- and BTG-treated anti-TNP-BSA IgM, large-scale bulk-purified IgM, and purified IgM that eluted from the MBL resin were also immobilized directly at 120 ng/well. MBL was incubated at 20 ng/well for 1 h and then sequentially with anti-MBL antiserum and alkaline phosphatase-conjugated anti-rabbit monoclonal IgG (γ chain-specific) as described by Arnold *et al.* (32). The assay was developed with the sensitive 4-methylumbelliferyl phosphate substrate, and the fluorescence was measured at λ_{ex} = 355 nm and λ_{em} = 460 nm after 1 h. The *bars* show mean MBL binding ± S.D. EDTA was used in negative controls, and the EDTA readings were subtracted from the results.

GlcNAc. No glycans were detected on the light chain of IgM by NP-HPLC (data not shown).

This is the first study of the IgM J chain *N*-linked glycans that occupy the single *N*-linked glycosylation site. The glycans identified all terminated in galactose or sialic acid, indicating that the J chain is fully exposed for glycan processing (Table II). The J chain *N*-linked glycans of secretory IgA have been identified by Royle *et al.* (47) and are occupied by similar glycan structures identified in IgM, indicating that secretory IgA and IgM follow the same pathway of polymerization and J chain attachment.

Based on the proportion of oligomannose identified, we conclude that Asn-402 is fully occupied and that Asn-563 has an occupancy of only 17% in this pooled normal human serum IgM sample. The proximity of the Asn-563 site to the CH4 domain has been suggested to make Asn-563 a poor substrate for oligosaccharyltransferase, the enzyme that attaches the $GlcNAc_2Man_9Glc_3$ structure to Asn of the *N*-linked glycosyla-

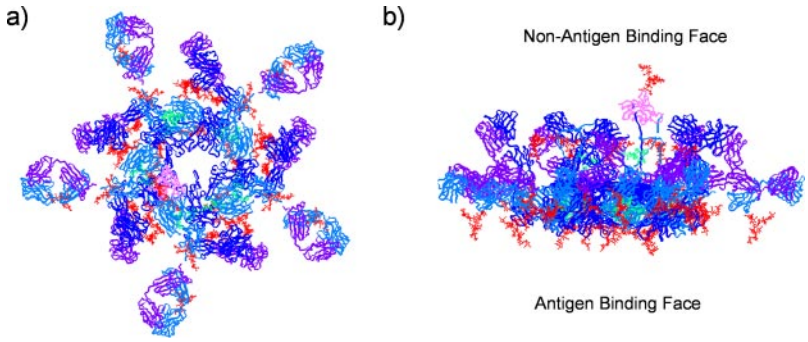

FIG. 7. **Molecular model of the glycosylated IgM pentamer with a glycosylated J chain.** The model of pentameric IgM (see "Experimental Procedures") shows the non-antigen-binding face (*a*) and a 90° rotation (*b*). The heavy chains are shown in *blue*; the light chains are shown in *dark purple*; and the J chain is shown in *light purple*. The complex glycans ($FcGlcNAc_2A_2BG_2S_2$ attached to Asn-171, Asn-332, and Asn-395) are shown in *red*. The oligomannose glycans ($GlcNAc_2Man_5$ attached to Asn-402 and $GlcNAc_2Man_8$ attached to Asn-563 at ~17% occupancy) are shown in *green*.

tion site in the endoplasmic reticulum (55).

Pentameric IgM Model—To form the IgM pentamer (Fig. 7), the monomers adopt a barrel-like structure rather than a planar structure. The IgM monomers are sterically unable to form a planar pentamer, but they can form a planar hexamer structure (data not shown). The pentameric IgM model suggests that IgM has two distinct faces, only one of which can bind to antigen because of the J chain, which projects from the non-antigen-binding face (Fig. 7*b*), and because of the barrel-like monomer arrangement. This would not be true for hexameric IgM, as the absence of a J chain and the planar arrangement would allow the Fab domains to flip between the two faces of the hexamer.

The antigen-binding face of pentameric IgM presents a large surface of complex glycans (Fig. 7*b*). IgM may bind to microorganisms via these glycan epitopes as an alternative route of antigen binding (other than through the Fab V regions). Influenza viruses initiate infection by binding the viral hemagglutinin to sialic acid on the cell surface (56, 57). IgM has 80.7% of its complex glycan pool terminating in sialic acid, which could allow IgM to bind to hemagglutinin, neutralizing the virus. Glycans with one or two terminal galactose residues account for 83.7% of the complex glycan pool and are a potential ligand for the asialoglycoprotein receptor, which binds to terminal galactose residues on serum glycoproteins. Upon binding, the asialoglycoprotein receptor conveys the ligand for intracellular degradation and is proposed to be involved in the clearance of IgA from the blood (58). Once pentameric IgM has bound antigen, these complex glycans on the antigen-binding face (Fig. 7*b*) appear to become inaccessible (Fig. 6). This is consistent both with the molecular model and with experimental data as discussed below. This may slow the clearance of IgM via receptors such as the asialoglycoprotein receptor and promote antigen-bound IgM to activate complement, as with the previously characterized C1q interaction (31).

MBL Binding to IgM—The glycans from normal total human serum IgM and those from IgM that eluted from an MBL-conjugated resin have been compared (Fig. 5 and Table III, parts A and B). The oligomannose structures that occupy normal serum IgM Asn-402 are similar in structure to those that occupy the homologous site in serum IgE (Asn-394) (32). MBL does not bind the oligomannose structures in serum IgE, as the additional CH2 hinge domain blocks access to these glycans (32).

This study has suggested that the occupancy of the normal human IgM Asn-563 site may be as little as 17%. Therefore, human serum IgM contains, on average, only one or two oligomannose sugars at the Asn-563 sites in each pentameric IgM molecule. The low number of potential ligands at this site does not present a binding surface to which MBL can bind with high avidity (Fig. 6). Oligomannose structures identified from pooled normal human serum IgM (23.4% of the glycan pool) were shown to be increased slightly to 25.3% in IgM eluted from the MBL resin. There were 43.7% more $GlcNAc_2Man_8$ structures occupying IgM eluted from the MBL-conjugated resin compared with normal serum IgM. $GlcNAc_2Man_8$ predominantly occupies the tail piece Asn-563 (3, 12). IgM that bound to the MBL resin had 26.4% of the Asn-563 sites occupied (two or three oligomannose structures at Asn-563 in each pentamer). We conclude that pooled normal human serum IgM does not have enough oligomannose occupying Asn-563 for MBL binding (which needs multiple glycan ligands) to give rise to high avidity binding. The occupancy of the Asn-563 site may be higher in lower vertebrates, as MBL has been shown to bind murine IgM (27). Glycan analysis of murine myeloma IgM has shown Asn-563 to have an occupancy of 44% (four to five accessible oligomannoses/pentamer at the tail piece glycosylation site) and human-mouse hybridoma IgM to have 42.5% hybrid structures at Asn-171 (compared with 3.3% in the total glycan pool of human serum IgM) (54).

In MBL-binding IgM, there was an increase in GlcNAc-terminating and hybrid structures (Table III, part A) from 7.5

TABLE III
N-Linked glycans that can potentially bind MBL: comparison of frequency in normal human IgM and IgM eluted from the MBL column

See the legend to Fig. 3 for explanation of glycan nomenclature.

Part A, the calculated occupancy of Asn-171, Asn-332, and Asn-395 with glycans that have terminal GlcNAc or mannose residues on the hybrid structures that are potential ligands for MBL. Data are from both pooled serum IgM and IgM eluted from the MBL resin. Values were calculated to account for the occupancy of Asn-171, Asn-332, and Asn-395 ((% glycan in pool % total IgM complex glycan in pool) × 100%). Part B, the calculated occupancy of Asn-402 and Asn-563 with oligomannose glycans that occupy only these sites. Data are from both pooled serum IgM and IgM eluted from the MBL resin (complete occupancy would produce 40% of the glycan pool as oligomannose structures, two of five *N*-linked glycosylation sites. Values were calculated to account for the occupancy of the two sites. Complete occupancy of both Asn-402 and Asn-563 would total 100% (% oligomannose glycan in pool/40% × 100%).

Occupying	Glycan	Pooled IgM	IgM eluted from MBL resin	Increase
		%	%	%
A. Asn-171, Asn-332, and/or Asn-395	$GlcNAc_2A_1$	1.0	3.7	208.3
	$GlcNAc_2A_2$	0.5	1.0	100.0
	$GlcNAc_2A_2B$	1.6	4.0	150.0
	$FcGlcNAc_2A_2$	0.3	0.3	0.0
	$GlcNAc_2A_3$	0.3	0.3	0.0
	$FcGlcNAc_2A_2B$	0.3	0.4	33.3
	$GlcNAc_2A_1Man_4G_1$	0.9	1.9	111.1
	$GlcNAc_2A_1Man_4G_1S_1$	2.4	3.2	33.3
	Total	7.5	14.8	97.3
B. Asn-402 and/ Asn-563	$GlcNAc_2Man_5$	14.0	14.3	2.1
	$GlcNAc_2Man_6$	23.8	21.0	−11.8
	$GlcNAc_2Man_7$	8.0	10.8	35.0
	$GlcNAc_2Man_8$	10.3	14.8	43.7
	$GlcNAc_2Man_9$	2.5	2.3	−8.0
	Total	58.6	63.2	7.8

to 14.8% at the complex glycan-occupied sites Asn-171, Asn-332, and Asn-395. MBL is able to interact with GlcNAc-terminating structures in a similar manner to the interaction that is seen upon IgG-G0 binding. A small population of hybrid structures $GlcNAc_2A_1Man_4G_1$ and $GlcNAc_2A_1Man_4G_1S_1$ was also identified; these structures were increased in IgM eluted from the MBL resin by 111.1 and 33.3%, respectively. Hybrid-type structures have been shown to occupy only Asn-171 in human-mouse heterohybridoma human IgM, accounting for 42.5% occupancy of the site (54). On average, there are four to five hybrid structures/IgM pentamer.

Pentameric IgM has 10 μ chains. From the glycan analysis, each normal human serum IgM contains, on average, 2.3 GlcNAc-terminating/hybrid structures on each pentamer (Table III). As expected, directly immobilized bulk serum IgM showed poor MBL binding (Fig. 6). MBL is likely to require more than two ligand glycan structures to bind with a high enough avidity to be detected in the assays used or to trigger biological function. Directly bound IgM isolated from the MBL resin bound MBL much better (Fig. 6). IgM that eluted from the MBL resin had, on average, 4.4 GlcNAc-terminating/hybrid structures on each pentamer. The subset of IgM to which MBL bound composed 20% of total serum IgM.

To establish whether these identified oligomannose and GlcNAc-terminating glycans are "presented" or "hidden" upon antigen binding by IgM, antigen-specific IgM was isolated. Anti-TNP-BSA IgM was tested both by binding it to the plate via antigen and by binding it directly (Fig. 6). The IgM preparation was digested with the exoglycosidases ABS and BTG to maximize the number of GlcNAc-terminating structures. The molecular model of pentameric IgM suggests that IgM has two distinct faces, only one of which can bind antigen. The complex glycans (including the GlcNAc-terminating structures) that cover the antigen-binding face of IgM (Fig. 7*b*) became inaccessible once IgM had bound antigen (Fig. 6). As expected, directly bound anti-TNP-BSA IgM bound MBL, but the antigen-bound form had very low MBL binding. This confirms, by experimentation, that, upon antigen binding, potential MBL-binding glycans become inaccessible. Antigen-bound IgM pentamers therefore do not activate complement via the lectin pathway, but MBL might have a role in the clearance of aggregated IgM.

Acknowledgments—We thank Dr. T. Butters for supplying glucosidase II and A. C. Willis for help with protein mass spectroscopy.

REFERENCES

1. Randall, T. D., King, L. B., and Corley, R. B. (1990) *Eur. J. Immunol.* **20,** 1971–1979
2. Wiersma, E. J., and Shulman, M. J. (1995) *J. Immunol.* **154,** 5265–5272
3. Wormald, M. R., Wooten, E. W., Bazzo, R., Edge, C. J., Feinstein, A., Rademacher, T. W., and Dwek, R. A. (1991) *Eur. J. Biochem.* **198,** 131–139
4. Baker, M. D., Wu, G. E., Toone, W. M., Murialdo, H., Davis, A. C., and Shulman, M. J. (1986) *J. Immunol.* **137,** 1724–1728
5. Mestecky, J., and Schrohenloher, R. E. (1974) *Nature* **249,** 650–652
6. Chapuis, R. M., and Koshland, M. E. (1974) *Proc. Natl. Acad. Sci. U. S. A.* **71,** 657–661
7. Frutiger, S., Hughes, G. J., Paquet, N., Luthy, R., and Jaton, J. C. (1992) *Biochemistry* **31,** 12643–12647
8. Randall, T. D., Brewer, J. W., and Corley, R. B. (1992) *J. Biol. Chem.* **267,** 18002–18007
9. Brandtzaeg, P., and Prydz, H. (1984) *Nature* **311,** 71–73
10. Sitia, R., Rubartelli, A., and Hammerling, U. (1984) *Mol. Immunol.* **21,** 709–719
11. Chapman, A., and Kornfeld, R. (1979) *J. Biol. Chem.* **254,** 824–828
12. Chapman, A., and Kornfeld, R. (1979) *J. Biol. Chem.* **254,** 816–823
13. Malhotra, R., Haurum, J., Thiel, S., and Sim, R. B. (1992) *Eur. J. Immunol.* **22,** 1437–1445
14. Weis, W. I., Drickamer, K., and Hendrickson, W. A. (1992) *Nature* **360,** 127–134
15. Turner, M. W. (1996) *Immunol. Today* **17,** 532–540
16. Holmskov, U., Malhotra, R., Sim, R. B., and Jensenius, J. C. (1994) *Immunol. Today* **15,** 67–74
17. Iobst, S. T., and Drickamer, K. (1994) *J. Biol. Chem.* **269,** 15512–15519
18. Vorup-Jensen, T., Petersen, S. V., Hansen, A. G., Poulsen, K., Schwaeble, W., Sim, R. B., Reid, K. B., Davis, S. J., Thiel, S., and Jensenius, J. C. (2000) *J. Immunol.* **165,** 2093–2100
19. Hajela, K., Kojima, M., Ambrus, G., Wong, K. H., Moffatt, B. E., Ferluga, J., Hajela, S., Gal, P., and Sim, R. B. (2002) *Immunobiology* **205,** 467–475
20. Matsushita, M., and Fujita, T. (1992) *J. Exp. Med.* **176,** 1497–1502
21. Thiel, S., Vorup-Jensen, T., Stover, C. M., Schwaeble, W., Laursen, S. B., Poulsen, K., Willis, A. C., Eggleton, P., Hansen, S., Holmskov, U., Reid, K. B., and Jensenius, J. C. (1997) *Nature* **386,** 506–510
22. Dahl, M. R., Thiel, S., Matsushita, M., Fujita, T., Willis, A. C., Christensen, T., Vorup-Jensen, T., and Jensenius, J. C. (2001) *Immunity* **15,** 127–135
23. Malhotra, R., Wormald, M. R., Rudd, P. M., Fischer, P. B., Dwek, R. A., and Sim, R. B. (1995) *Nat. Med.* **1,** 237–243
24. Butler, M., Quelhas, D., Critchley, A. J., Carchon, H., Hebestreit, H. F., Hibbert, R. G., Vilarinho, L., Teles, E., Matthijs, G., Schollen, E., Argibay, P., Harvey, D. J., Dwek, R. A., Jaeken, J., and Rudd, P. M. (2003) *Glycobiology* **13,** 601–622
25. Roos, A., Bouwman, L. H., van Gijlswijk-Janssen, D. J., Faber-Krol, M. C., Stahl, G. L., and Daha, M. R. (2001) *J. Immunol.* **167,** 2861–2868
26. Roos, A., Bouwman, L. H., Munoz, J., Zuiverloon, T., Faber-Krol, M. C., Fallaux-van den Houten, F. C., Klar-Mohamad, N., Hack, C. E., Tilanus, M. G., and Daha, M. R. (2003) *Mol. Immunol.* **39,** 655–668
27. Nevens, J. R., Mallia, A. K., Wendt, M. W., and Smith, P. K. (1992) *J. Chromatogr.* **597,** 247–256
28. Koppel, R., and Solomon, B. (2001) *J. Biochem. Biophys. Methods* **49,** 641–647
29. Davis, A. C., Roux, K. H., and Shulman, M. J. (1988) *Eur. J. Immunol.* **18,** 1001–1008
30. Collins, C., Tsui, F. W., and Shulman, M. J. (2002) *Eur. J. Immunol.* **32,** 1802–1810
31. Perkins, S. J., Nealis, A. S., Sutton, B. J., and Feinstein, A. (1991) *J. Mol. Biol.* **221,** 1345–1366
32. Arnold, J. N., Radcliffe, C. M., Wormald, M. R., Royle, L., Harvey, D. J., Crispin, M., Dwek, R. A., Sim, R. B., and Rudd, P. M. (2004) *J. Immunol.* **173,** 6831–6840
33. Wessel, D., and Flugge, U. I. (1984) *Anal. Biochem.* **138,** 141–143
34. Johnstone, A., and Thorpe, R. (1987) *Immunochemistry in Practice*, 2nd Ed., Blackwell Scientific Publications, Oxford, UK
35. Sim, R. B., Day, A. J., Moffatt, B. E., and Fontaine, M. (1993) *Methods Enzymol.* **223,** 13–35
36. Küster, B., Wheeler, S. F., Hunter, A. P., Dwek, R. A., and Harvey, D. J. (1997) *Anal. Biochem.* **250,** 82–101
37. Radcliffe, C. M., Diedrich, G., Harvey, D. J., Dwek, R. A., Cresswell, P., and Rudd, P. M. (2002) *J. Biol. Chem.* **277,** 46415–46423
38. Bigge, J. C., Patel, T. P., Bruce, J. A., Goulding, P. N., Charles, S. M., and Parekh, R. B. (1995) *Anal. Biochem.* **230,** 229–238
39. Guile, G. R., Rudd, P. M., Wing, D. R., Prime, S. B., and Dwek, R. A. (1996) *Anal. Biochem.* **240,** 210–226
40. Zamze, S., Harvey, D. J., Chen, Y. J., Guile, G. R., Dwek, R. A., and Wing, D. R. (1998) *Eur. J. Biochem.* **258,** 243–270
41. Royle, L., Mattu, T. S., Hart, E., Langridge, J. I., Merry, A. H., Murphy, N., Harvey, D. J., Dwek, R. A., and Rudd, P. M. (2002) *Anal. Biochem.* **304,** 70–90
42. Tan, S. M., Chung, M. C., Kon, O. L., Thiel, S., Lee, S. H., and Lu, J. (1996) *Biochem. J.* **319,** 329–332
43. Pearson, W. R., Wood, T., Zhang, Z., and Miller, W. (1997) *Genomics* **46,** 24–36
44. Berman, H. M., Westbrook, J., Feng, Z., Gilliland, G., Bhat, T. N., Weissig, H., Shindyalov, I. N., and Bourne, P. E. (2000) *Nucleic Acids Res.* **28,** 235–242
45. Wan, T., Beavil, R. L., Fabiane, S. M., Beavil, A. J., Sohi, M. K., Keown, M., Young, R. J., Henry, A. J., Owens, R. J., Gould, H. J., and Sutton, B. J. (2002) *Nat. Immunol.* **3,** 681–686
46. Stanfield, R. L., Fieser, T. M., Lerner, R. A., and Wilson, I. A. (1990) *Science* **248,** 712–719
47. Royle, L., Roos, A., Harvey, D. J., Wormald, M. R., van Gijlswijk-Janssen, D., Redwan, E.-R. M., Wilson, I. A., Daha, M. R., Dwek, R. A., and Rudd, P. M. (2003) *J. Biol. Chem.* **278,** 20140–20153
48. Petrescu, A. J., Petrescu, S. M., Dwek, R. A., and Wormald, M. R. (1999) *Glycobiology* **9,** 343–352
49. Wormald, M. R., Petrescu, A. J., Pao, Y. L., Glithero, A., Elliott, T., and Dwek, R. A. (2002) *Chem. Rev.* **102,** 371–386
50. Petrescu, A. J., Milac, A. L., Petrescu, S. M., Dwek, R. A., and Wormald, M. R. (2004) *Glycobiology* **14,** 103–114
51. Monica, T. J., Williams, S. B., Goochee, C. F., and Maiorella, B. L. (1995) *Glycobiology* **5,** 175–185
52. Anderson, D. R., Samaraweera, P., and Grimes, W. J. (1983) *Biochem. Biophys. Res. Commun.* **116,** 771–776
53. Fukuta, K., Abe, R., Yokomatsu, T., Kono, N., Nagatomi, Y., Asanagi, M., Shimazaki, Y., and Makino, T. (2000) *Arch. Biochem. Biophys.* **378,** 142–150
54. Leibiger, H., Kersten, B., Albersheim, P., and Darvill, A. (1998) *Glycobiology* **8,** 497–507
55. Nilsson, I. M., and von Heijne, G. (1993) *J. Biol. Chem.* **268,** 5798–5801
56. Gottschalk, A. (1957) *Biochim. Biophys. Acta* **23,** 645–646
57. Wu, W., and Air, G. M. (2004) *Virology* **325,** 340–350
58. Stockert, R. J. (1995) *Physiol. Rev.* **75,** 591–609